

# Structural and magnetic properties of nanoclusters formed in III-V semiconductors

Krystyna Lawniczak-Jablonska<sup>1\*</sup>, Anna Wolska<sup>1</sup> and Marcin T. Klepka<sup>1</sup>

<sup>1</sup>Institute of Physics, Polish Academy of Science, Al. Lotnikow 32/46, 02-668  
Warsaw, Poland

\*E-mail: jablo@ifpan.edu.pl

**Abstract.** Studies of X-ray magnetic circular dichroism (XMCD) were performed for a set of GaMnAs films with different Mn concentrations priorly and after high temperature annealing (500 and 600 °C). After thermal treatment, GaMnAs samples with zinc blende structure and MnAs hexagonal nano-clusters were formed. In most of the samples, both types of clusters were detected by EXAFS studies. Dependence of the orbital and the spin moments on magnetic field were calculated from XMCD data by applying the sum rule. It was shown that both moments were much larger for MnAs nano-clusters. When these inclusions are formed even in a small amount, they dominate the XMCD signal. Interestingly, in some of samples the zinc blende GaMnAs nano-clusters were observed at a surface while in the bulk of hexagonal MnAs. Therefore, the location of magnetic ions in the host matrix is crucial for their magnetic properties. This unique information can be provided by XAS and XMCD.

## 1. Introduction

Magnetic semiconductors have attracted considerable attention due to expectation that manipulation of an electron spin, as an alternative to manipulation of an electron charge, can be used for the storage of information in semiconducting devices. In spite of the efforts of many technologists and scientists, until now the magnetic semiconductors with uniformly distributed magnetic ions do not exhibit ferromagnetic properties at room temperature. The highest solubility limit reported for  $\text{Ga}_{1-x}\text{Mn}_x\text{As}$  is around  $x=0.1$  [1]. Therefore, there is an increasing interest in granular materials. Presence of magnetically active metallic nanoclusters in GaMnAs leads to enhanced magnetotransport [2] and magneto-optical [3] properties over a wide spectral range. This phenomenon opens an opportunity for various applications of such hybrid systems. Location of magnetic ions in the host matrix is crucial for magnetic properties and is correlated with all other important physical properties. Moreover, an understanding of the local environment of magnetic ions in semiconductors and its valence state has an important impact on optimization of material properties. Information about the atom location in the crystal lattice is provided by only a few techniques. Among them, EXAFS is a well-established tool which has been proven to be useful as a chemically sensitive local probe for identification of the site and the valence state of magnetic ions in DMSs [4]. The calculated XANES and EXAFS spectra for models with different location of magnetic ions in the crystal structure, under assumption that all ions are located only in the given position, show significant differences [5-8]. The quantitative comparison of the calculated model spectra with the measured spectra, is a procedure for a quick check of homogeneity. It is known that, in the as-grown MBE samples of the GaAs matrix, the Mn atoms may occupy substitutional and interstitial positions, but the abundance of each position is not easy to find. The number of Mn atoms in the interstitial positions is increasing with the Mn concentration. In our earlier paper we demonstrated, how the proportion between these two locations can be estimated applying EXAFS and XANES [8].

Two kinds of nanoclusters existing in the GaMnAs samples have been reported: cubic zinc blende (ZB) and hexagonal MnAs phases [e.g. 9]. The formation of nanoclusters in the MBE as grown GaMnAs layers started during the annealing above 400 °C. Presence of these nanoclusters changes



drastically the magnetic properties of layers increasing additionally the  $T_C$  above RT. Creation of small and exclusively cubic MnAs clusters was assumed by annealing at 500 °C and larger hexagonal by annealing at 600 °C and above. Recently performed detailed EXAFS studies on a set of samples with different Mn concentration unambiguously demonstrated that such assumption is not justified [10, 11]. The problem is more complicated and depends on the location of Mn in as grown sample (interstitial or substitutional). Study of the atomic order around Mn atoms showed, that the ZB MnAs clusters do not exist because 12 Mn atoms in the second coordination sphere cannot be fitted to the experimental spectra. Instead, the study revealed that small cubic GaMnAs clusters are formed with much higher content of Mn than ever produced in GaMnAs layers with randomly distributed Mn atoms (about 20%) [10]. Clusters with the size larger than 8 nm have had already the MnAs hexagonal structure. In most of studied samples, the clusters with both structures were present. The proportion of Mn in each structure estimated by EXAFS was in perfect agreement with the size distribution of clusters found from TEM analysis [11]. Knowing the position of Mn ions in crystal structure it is very interesting to exam their magnetic properties. The x-ray magnetic circular dichroism (XMCD) is well established technique to perform such studies. In the present paper, the results of XMCD studies on a set of samples discussed in papers [10, 11] are reported.

## 2. Experimental

Sets of  $\text{Ga}_{1-x}\text{Mn}_x\text{As}$  layers with nominal Mn contents  $x = 0.015, 0.06, 0.07$ , and  $0.08$  were grown by MBE on the (001)-oriented GaAs substrates at the temperature of 230 °C. Nominal Mn concentrations were estimated from Mn/Ga flux ration. The thickness of layers was around 1  $\mu\text{m}$ . After deposition, each sample was cut into three pieces: one of them was left untreated (as grown), the remaining two were reintroduced into the MBE growth chamber and annealed under  $\text{As}_2$  flux for 30 min at  $T = 500$  °C and at  $T = 600$  °C, respectively. Details of samples growth and their characterisation are reported in refs [10, 11]. In table 1, results of EXAFS studies at the set of samples under consideration are collected. In most of samples, both kind of nanoclusters were found: GaMnAs ZB and hexagonal MnAs. In the sample with smallest Mn concentration ( $x=0.015$ ), only the GaMnAs ZB nanoclusters were detected.

**Table 1.** The percentage of Mn atoms in GaMnAs ZB clusters and in hexagonal MnAs clusters as estimated by EXAFS analysis.

Sample	Annealed at 500 °C		Annealed at 600 °C	
Clusters type	ZB	Hexagonal	ZB	Hexagonal
$x = 0.015$	100%	0	100%	0%
$x = 0.06$	72(2)%	28%	40(5) %	60%
$x = 0.07$	53(5)%	47%	15(5)%	85%
$x = 0.08$	69 (2)%	31%	50(5)%	50%

XMCD studies were performed at ESRF ID08 beamline on the  $L_{2,3}$  Mn edge in the function of the temperature and magnetic field. Although, the best mode of XMCD detection is the transmission, the total electron yield (TEY) and the total fluorescence yield (TFY) were simultaneously applied for spectra recording because samples were thin films deposited on a thick substrate. One should be aware that TEY method can be sensitive to variable magnetic field and changes in electron detecting efficiency (photocurrent). The TFY is insensitive to the applied field, but the yield is intrinsically not proportional to the absorption cross section because the radiative to non-radiative relative core-hole

decay probability depends strongly on symmetry and spin polarization of the XAS final states. These two detection modes differ also in the examined depth (TEY surface, TFY bulk) and can provide different result in the case of inhomogeneous samples.

As an example in the figure 1a XMCD spectra for the sample with nominal content of  $\text{Mn}=0.08$  annealed at  $600^\circ\text{C}$  is shown. Measurements were performed at room temperature and in 5T magnetic field, simultaneously with above two detection modes. The shape of the XMCD is very different for each of modes. This is an additional confirmation that two kinds of Mn locations in this sample exist as was already reported from EXAFS studies [10] and is shown in the table 1. The XMCD signal registered by TEY is characteristic for the cubic ZB atomic order around Mn as was reported in several papers [e.g. 12]. The XMCD recorded by TFY is characteristic for octahedral symmetry of atomic arrangement as in hexagonal MnAs clusters [13 and references therein]. This indicates that Mn atoms have cubic arrangement at the surface and can be located in substitutional position either in the GaAs matrix or cubic  $\text{Ga}_{1-x}\text{Mn}_x\text{As}$  clusters and in the bulk of sample hexagonal MnAs clusters dominate. It is worth notice that XMCD for hexagonal clusters is almost one order of magnitude larger than for cubic clusters. In the case of the sample with  $x=0.015$  annealed at  $500^\circ\text{C}$  (figure 1b), where only cubic nano-clusters were reported from EXAFS analysis (see table 1), no significant difference between both modes of detection was observed. Therefore, performing the XMCD analysis one should pay special attention to the used mode of detection. For detailed analysis of XMCD, the TFY measurements were taken because bulk properties of samples were of interest.

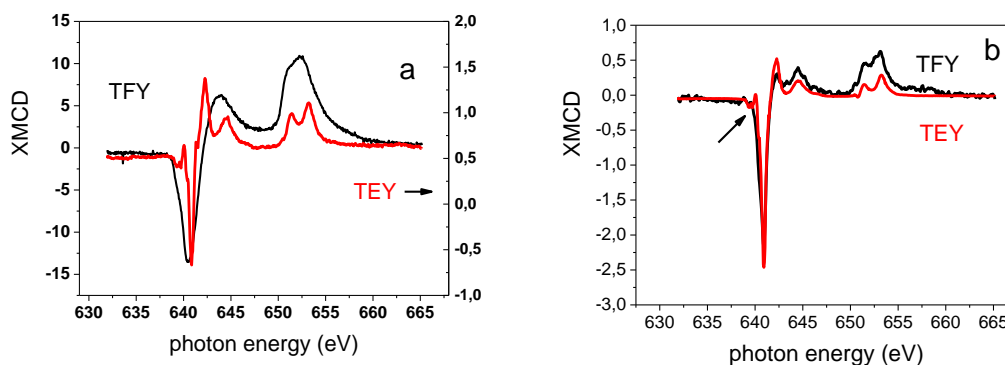


**Figure 1.** XMCD spectra measured with TEY (red) and TFY (black) detection mode, for samples  $\text{Ga}_{1-x}\text{Mn}_x\text{As}$  with a)  $x=0.08$  and b)  $x=0.015$  Mn content. The measurements performed at room temperature and 5T magnetic field.

The quantitative evaluation of magnetic moments, separated into the spin and the orbital contributions, was performed from integrals over XMCD spectra by applying the so-called sum rules [14,15]. In the numerical evaluation of the orbital and the spin moments in the case of transition metals and particularly Mn atoms, two main sources of errors are expected. First is the coupling between  $L_2$  and  $L_3$  edges (so called branching ratio) which influences spin moment. It was predicted that the intermixing of the  $L_2$  and  $L_3$  absorption edges is mainly present in the early transition metals [16] where the electron core hole interaction increases while the spin-orbit splitting decreases. For such metals (e.g. Mn) the application of the spin sum rule can produce an error up to 30%. Error at this level is indicated in numerical values presented in table 2 and treated as confidence interval for revealing the trends in the changes of magnetic orbital and spin moment. Second possible source of errors in applying the spin sum rule is the energy dependent radial matrix elements [17]. Although the sum rules are normalized to the isotropic absorption cross-section, which is proportional to the number

of holes in the d-shell, also the continuum states contribute. In the performed calculation, the number of holes in the d-shell was set equal to 4.8, similarly as in numerous other papers, reported XMCD for  $\text{Ga}_{1-x}\text{Mn}_x\text{As}$  [e.g. 12]. To eliminate contribution from continuum states, a double step function was fitted to the absorption spectrum and subtracted. This procedure is likely to introduce a systematic error in the determination of a number of holes in the final state. Therefore, not the numerical values but the observed relative changes of the orbital and the spin magnetic moments in the function of magnetic field and the structure of samples will be rather discussed.

### 3. Results and discussion

Quantitative results of the XMCD spectra analysis for samples with  $x=0.015$  are shown in the figure 2 for as grown and annealed in 500 °C samples. Spectra were measured at 150 K as a function of magnetic field. Without magnetic field at this temperature, no XMCD signal was detected. In the as grown sample similar as in other reports [e.g. 12], the small orbital moment was detected, whose absolute value increased with the magnetic field from  $-0.0012 \mu_B$  at 0.5T to  $-0.02 \mu_B$  at 5T and  $T=150$  K. The orbital moment was not changing noticeably, when cubic clusters were formed after 500 °C annealing (table 2 and figure 2). Starting from 2T, the orbital moment was found not to depend significantly on the magnetic field as can be seen in figure 2b and table 2. Interestingly, the orientation of the orbital to the spin moment changes in these two samples depending on the magnetic field. For the as grown sample, the parallel orientation was observed at 1 and 2 T, but for 500 °C annealed sample only for 1 T magnetic field. For all other cases, antiparallel orientation was found. The reason for the observed changes needs more detailed studies.

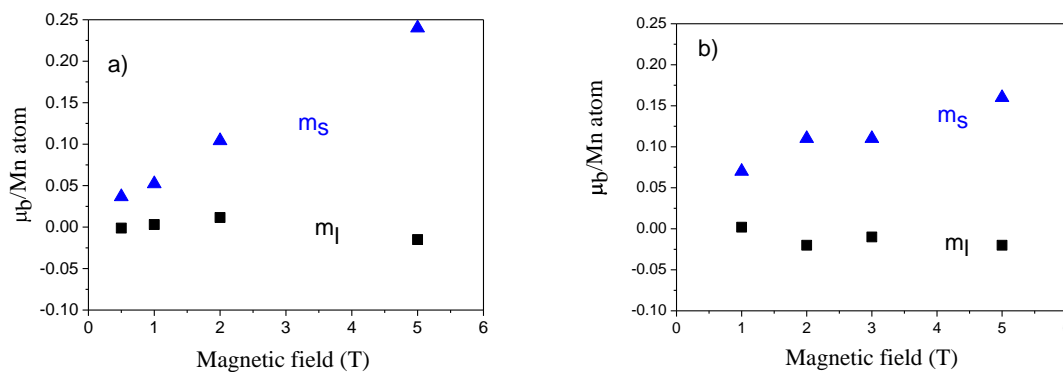


**Figure 2.** The field dependency of the spin (triangles) and orbital (squares) of the magnetic moments estimated from the XMCD measurements for  $\text{Ga}_{1-x}\text{Mn}_x\text{As}$  for  $x=0.015$  a) as grown samples; b) after annealing at 500 °C.

The value of the spin moment changes with the magnetic field depending on the kind of samples. In the as grown sample, similarly as it was reported for solid solution of Mn in GaAs [12], the spin moment increases linearly with the magnetic field (figure 2a). For the annealed film (500 °C) with small ( $\sim 5\text{nm}$ ) cubic nano-clusters, the XMCD signal initially increases rapidly and the spin moment increases by 57% on increasing the field from 1 to 2 T, then remains constant in the limit of error (saturates) indicating the magnetic coupling of Mn ions (figure 2b table 2). This effect is more pronounced in the sample with still small but already hexagonal MnAs nano-clusters (figure 3, table 2). When the hexagonal MnAs nano-clusters are formed, the strong magnetic coupling between Mn ions can be observed already at 150 K. The saturation is reached at 0.5 T and no change of the orbital and spin moment with the increase of magnetic field is observed. Both moments are antiparallel

coupled in the whole range of magnetic field. The XMCD is observed already at 0.05T with quite large orbital and spin moments.

**Table 2.** The value of the orbital  $m_l$  and the spin  $m_s$  magnetic moment for  $\text{Ga}_{1-x}\text{Mn}_x\text{As}$  samples with  $x=0.015$  after different thermal treatment measured at 150 K in the function of magnetic field.

Sample/ moment	0.05T	0.1T	0.5T	1T	2T	3T	5T
as grown							
$m_l (\mu_b)$			-0.0012(4)	0.0030(6)	0.012(4)		-0.020(6)
$m_s (\mu_b)$			0.04(1)	0.05(1)	0.11(4)		0.24(7)
an. 500 °C							
$m_l (\mu_b)$				0.0020(6)	-0.020(6)	-0.013(4)	-0.020(6)
$m_s (\mu_b)$				0.07(2)	0.11(4)	0.11(4)	0.16(5)
an. 600 °C							
$m_l (\mu_b)$	-0.020(6)	-0.09(3)	-0.20(6)	-0.25(7)	-0.26(7)		-0.20(6)
$m_s (\mu_b)$	0.15(4)	0.28(9)	0.64(21)	0.77(25)	0.79(26)		0.82 (27)

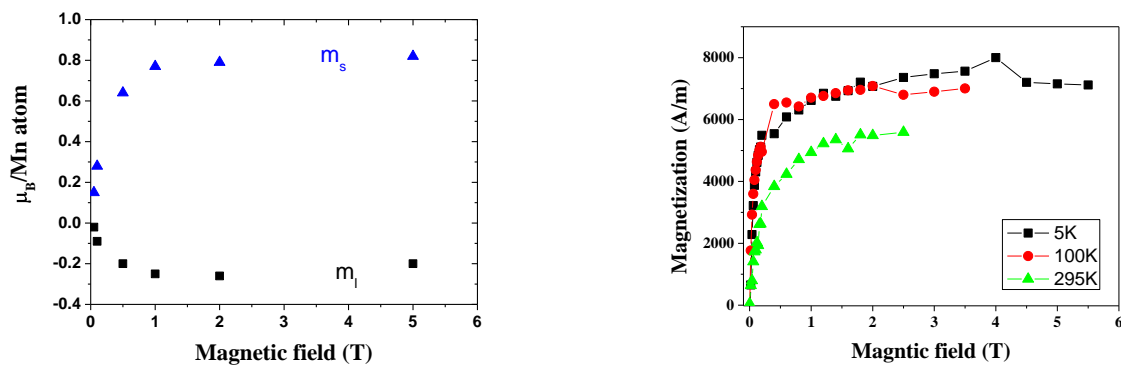


**Figure 3.** The field dependence of the spin (triangles) and the orbital (squares) magnetic moments estimated from the XMCD measurements for  $\text{Ga}_{1-x}\text{Mn}_x\text{As}$  film with  $x=0.015$  after annealing at 600 °C (left). The field dependence of magnetization measured by SQUID performed for the same sample at different temperatures (adapted from paper [11] right).

Measurements of the superconducting quantum interference device (SQUID) magnetization (figure 3 right) performed for the same sample, after the correction on diamagnetic compound typical for GaAs, show also typical ferromagnetic-like behavior (i.e. very fast saturation with magnetic field) even at 295 K, in agreement with magnetic properties of bulk MnAs. These both findings confirmed that when MnAs hexagonal nano-cluster are formed even in small amount which was not detected by EXAFS (table1), XRD or TEM, they dominate the magnetic signal.

## Acknowledgments:

Financial support from the EU FP7 EAgLE project under the grant agreement REGPOT-CT-2013-316014 is gratefully acknowledged. The authors would like to thank Violetta Sessi for help during the measurements at ESRF.

## References

- [1] Mack S, Myers R C, Heron J T, Gossard A C, and Awschalom D D 2008 *Appl. Phys. Lett.* **92** 192502
- [2] Ye S, Klar P J, Hartmann Th, Heimbrodt W, Lampalzer M, nau S, Torunski T, Stolz W, Kurz T, Krug von Nidda H-A, Loidi A 2003 *Appl. Phys. Lett.* **83** 3927
- [3] Yokoyama M, Yamaguchi H, Ogawa T and Tanaka M 2005 *J. Appl. Phys.* **97**, 10D317
- [4] Lawniczak-Jablonska K, 2015 Chapter 15, Magnetic Ions in Group III–V Semiconductors, Springer-Verlag Berlin Heidelberg 2015, C.S. Schnohr and M.C. Ridgway (eds.), *X-Ray Absorption Spectroscopy of Semiconductors*, Springer Series in Optical Sciences 190
- [5] Shioda R, Ando K, Hayashi T, and Tanaka M 1998 *Phys. Rev. B* **58**, 1100
- [6] Bacewicz R, Twarog A, Malinowska A, Wojtowicz T, Liu X, Furdyna J K 2005 *J. Phys. Chem. Solids* **66** 2004
- [7] Demchenko I N, Lawniczak-Jablonska K, Story T, Osinniy V, Jakiela R, Domagala J Z, Sadowski J, Klepka M, Wolska A, Chernyshova M, 2007 *J. Phys: Condens. Matter* **19** 496205
- [8] Lawniczak-Jablonska K, Libera J, Wolska A, Klepka M T, Jakiela R, J. Sadowski 2009 *Rad. Phys. Chem.* **78**, S80
- [9] Kwiatkowski A, Wasik D, Kaminska M, Bozek R, Szczytko J, Twardowski A, Borysiuk J, Sadowski J, Gosk J 2007 *J. Appl. Phys.* **101** 113912
- [10] Lawniczak-Jablonska K, Libera J, Wolska A, Klepka M T, Dluzewski P, Sadowski J, Wasik D, Twardowski A, Kwiatkowski A and Sato K 2011 *Phys. Stat. Sol. RRL* **5**, 62
- [11] Lawniczak-Jablonska K, Bak-Misiuk J, Dynowska E, Romanowski P, Domagala J Z, K, Libera J, Wolska A, Klepka M T, Dluzewski P, Sadowski J, Barcz A, Wasik D, Twardowski A, Kwiatkowski A 2011 *J. Solid State Chem.* **184**, 1530
- [12] Edmonds K W, Farley N R S, Johal T K, van der Laan G, Champion R P, Gallagher B L, and Foxon C T 2005 *Phys. Rev. B* **71**, 064418
- [13] Lawniczak-Jablonska K, Wolska A, Klepka M T, Kret S, Gosk J, Twardowski A, Wasik D, Kwiatkowski A, Kurowska B, Kowalski B J, Sadowski J 2011 *J. Appl. Phys.* **109**, 074308
- [14] Thole B T, Carra P, Sette F, van der Laan G 1992 *Phys. Rev. Lett.* **68**, 1943
- [15] Carra P, Thole B T, Altarelli M, Wang X 1993 *Phys. Rev. Lett.* **70**, 694
- [16] Schmitalla J and Ebert H 2005 comment in *Phys. Rev. Lett.* **80**, 4586
- [17] Wu R, Wang D and Freeman A J 1993 *Phys. Rev. Lett.* **71**, 3581